

Thermal roughening of an SOS-model with elastic interaction

Frank Gutheim, Heiner Müller-Krumbhaar, and Efim Brener
Forschungszentrum Jülich, D-52425 Jülich, Germany

Vladimir Kaganer

Paul-Drude-Institut für Festkörperelektronik, Hausvogteiplatz 5-7, D-10117 Berlin, Germany

We analyze the effects of a long-ranged step-step interaction on thermal roughening within the framework of a solid-on-solid model of a crystal surface by means of Monte Carlo simulation. A repulsive step-step interaction is modeled by elastic dipoles located on sites adjacent to the steps. In order to reduce the computational effort involved in calculating interaction energy based on long-ranged potentials, we employ a multi-grid scheme. As a result of the long-range character of the step interaction, the roughening temperature increases drastically compared to a system with short-range cutoff as a consequence of anti-correlations between surface defects.

I. INTRODUCTION

At low temperatures crystal surfaces are known to assume the shape of a plane facet. With increasing temperature fluctuations gradually contribute a nonzero thickness to the initially flat facet. This surface thickness finally diverges at a finite temperature, the roughening temperature, where the order of the facet is lost completely. This transition can be described by a set of renormalization group equations first analyzed by Kosterlitz and Thouless¹. Because of its unusual properties and the relation to the two-dimensional Coulomb gas², this roughening transition has attracted substantial attention^{3,4,5,6}.

Various discrete solid-on-solid models have been shown to undergo this type of transition. Most of these models incorporate local interactions, at most next-nearest neighbor interactions. Within some of these models a transition involving in-plane disorder is possible, usually referred to as preroughening^{7,8,9,10,11,12,13,14}. Step-step interaction by means of elastic deformation of the crystal, however, is of a long-ranged nature and has apparently not been previously studied in the context of roughening. Leaving the matter of preroughening aside, we will try to elucidate the effects of long-range elastic interactions on the roughening process.

The paper is organized as follows. First we will introduce elastic interaction between surface defects and suggest some simplifications to make the problem tractable. Then we present the details of our discrete solid-on-solid model allowing for long-range step interaction. We will show the results of our extensive Monte Carlo simulations and interpret the effects.

II. STEP INTERACTION

Elastic step interaction on the surface of a semi-infinite crystal can be described in terms of elastic force dipoles located at the step edges^{15,16,17,18}. Knowing the Green function G_{ij} for an infinite elastic half-space one is able to calculate the elastic displacement field $u_i(\mathbf{r})$ from a

given force density $f_i(\mathbf{r})$

$$u_i(\mathbf{r}) = \int d^2r' G_{ij}(\mathbf{r} - \mathbf{r}') f_j(\mathbf{r}'). \quad (1)$$

The elastic energy E_{el} becomes

$$\begin{aligned} E_{\text{el}} &= - \int d^2r u_i(\mathbf{r}) f_i(\mathbf{r}) \\ &= - \int \int d^2r d^2r' G_{ij}(\mathbf{r} - \mathbf{r}') f_j(\mathbf{r}') f_i(\mathbf{r}). \end{aligned} \quad (2)$$

Using that forces $f_i(\mathbf{r})$ are present only in the vicinity of a step and that the mono-pole moment at the step vanishes, we can rewrite the energy using force dipole densities $q_{ik}(\mathbf{r})$ as the next term in a multi-pole expansion

$$E_{\text{el}} \approx - \int \int d^2r d^2r' q_{jk}(\mathbf{r}') q_{il}(\mathbf{r}) \partial_k \partial_l G_{ij}(\mathbf{r} - \mathbf{r}'). \quad (3)$$

Using symmetry arguments one can determine two types of force dipoles that are considered to be present at a step¹⁶. One type involves in-plane forces perpendicular to the step, the other arises from forces orthogonal to the crystal surface. Due to the structure of the Green function, dipole tensors involving forces orthogonal to the surface show a behavior different from those involving only in-plane forces^{16,18}. The former lead to attractive or repulsive interaction depending on the signs of the steps, the latter produce a sign independent behavior, which is strictly repulsive. There are materials^{19,20} where the sign dependent contributions are small compared to the step repulsion caused by in-plane forces, and we will restrict our model to the case, where we can neglect sign dependence of the steps.

In the case of isotropic linear elasticity the half-space elastic Green function $G_{ij}(\mathbf{r})$ can be written in a simple form¹⁵

$$G_{ij}(\mathbf{r}) = \frac{1 + \sigma}{\pi E} \frac{1}{r} \left\{ (1 - \sigma) \delta_{ij} + \sigma \frac{r_i r_j}{r^2} \right\} \quad (4)$$

where i and j are restricted to in-plane coordinates.

For a step stretching in y -direction one would assume the force dipole tensor at the step to be of the type $q_{ij} \sim \delta_{ix}\delta_{jx}$. This means that the interaction between two line elements will depend on their orientation.

In the case of two parallel steps, a distance d in y -direction apart, the interaction energy density w (per area squared) can be computed by evaluating the integrand from eq. (3) for two interacting force dipoles of the type $q_{ij} = \delta_{ix}\delta_{jx}$. It is given by

$$w(r, \varphi) = \gamma \left[\frac{3 \cos \varphi - 1}{r^3} + \frac{\sigma}{1 - \sigma} \frac{2 + 15 \cos^4 \varphi - 15 \cos^2 \varphi}{r^3} \right] \quad (5)$$

where φ denotes the angle between the radius vector \mathbf{r} and the orientation of the dipole forces, which is given by $\varphi = \arctan(\Delta y/d)$, and Δy is the distance between the dipoles in y -direction. The factor γ is given by

$$\gamma = \frac{1 - \sigma^2}{\pi E} \tilde{Q}^2, \quad (6)$$

where $\tilde{Q} = Q/a$ is the dipole moment (per unit step length) and Q would be the dipole moment assigned to a single atom at the step edge.

Integrating the energy density for a configuration with two parallel steps at distance d , we state that the energy per unit length of the line is just

$$\tilde{W} = 4\gamma \frac{1}{d^2} - 2\gamma \frac{1}{\varepsilon^2} \frac{1 - 2\sigma}{1 - \sigma}, \quad (7)$$

where the interaction was limited to distances greater ε . Note that the second term, which contributes to line energy, is negative for all possible Poisson ratios $-1 \leq \sigma \leq 1/2$.

In order to make another simplification of the step-step interaction we compare the above result to the case of a scalar $w \sim 1/r^3$ interaction associated with isotropic dipoles $q_{ij} \sim \delta_{ij}$,

$$\tilde{W}_{\text{scalar}} = 4\gamma \frac{1}{d^2} + 2\gamma \frac{1}{\varepsilon^2}, \quad (8)$$

from which we conclude that the only difference in this specific geometry is a change in the line energy, which is mainly due to contributions from short range interactions.

Because we aim at showing the effect of long-range interactions on the thermal roughening process, we neglect the angular dependence completely and assume that the dipole moments are isotropic. This leads to a simple isotropic $1/r^3$ -interaction between force dipoles. Furthermore this ensures that the elastic contribution to the step energy is positive.

III. MODEL DESCRIPTION

Within the framework of a solid-on-solid model we describe the crystal surface by a simple height field of inte-

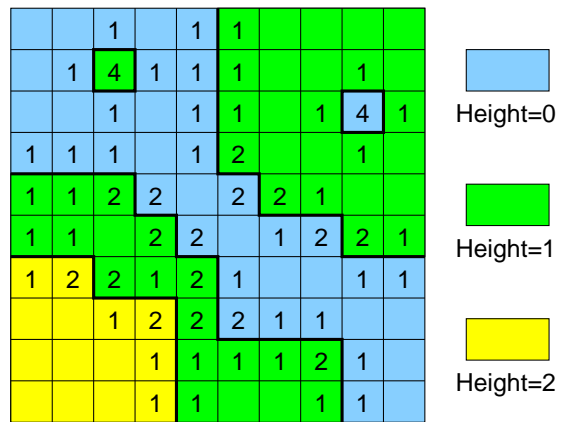


FIG. 1: The numbers of dipole charges assigned to a lattice sites is proportional to the accumulated absolute height difference corresponding to eq. 10.

ger numbers h . Like in a common SOS model, overhangs are forbidden. Instead of the usual surface energy term (summation over nearest neighbors)

$$E_{\text{surf}} = \frac{J}{2} \sum_{\langle i,j \rangle} |h_i - h_j|^\alpha, \quad (9)$$

with coupling constant J and $\alpha = 1, 2$ for the ASOS-model and the DGSOS-model respectively, we define an elastic step interaction by introducing a field of elastic dipole charges q . To every lattice site a dipole charge q_k proportional to the number of height differences to the four neighboring sites is assigned, i. e. site k carries a number of

$$q_k = \frac{1}{2} \sum_{\langle i,j \rangle} |h_i - h_j| \delta_{ik} \quad (10)$$

charges. Figure 1 gives an example how charges are assigned to a simple height field configuration. The elastic dipole charges interact, in consequence of eq. (8), via a modified r^{-3} interaction potential $\Psi(r)$,

$$\Psi(r) = \begin{cases} r^{-3} & \text{if } r \geq 1 \\ 1 & \text{if } r = 0 \end{cases}, \quad (11)$$

where r is the in-plane distance between two lattice sites measured in units of the lattice constant. This gives rise to the elastic energy

$$E_{\text{el}} = \frac{w_{\text{el}}}{2} \sum_{i,j} q_i q_j \Psi(r_{ij}), \quad (12)$$

where r_{ij} is the distance between lattice sites i and j and w_{el} can be adjusted to give the desired interaction strength. Note that the case $i = j$ is not excluded from the summation. During our simulation this constant had the value $w_{\text{el}} = 0.31$, which gives a line energy of about 0.5 per unit length for infinite range interaction.

Later we also limit the range of interaction. For this purpose we introduce a cutoff-potential Ψ_l with cutoff length l

$$\Psi_l(r) = \begin{cases} \Psi(r) & \text{if } r \leq l \\ 0 & \text{if } r > l \end{cases} \quad (13)$$

which vanishes for distances greater than l .

For two straight steps of length L with distance d this elastic energy contribution consists of the self energies of the steps and the expected $\sim d^{-2}$ step interaction term

$$E_{\text{int}} \sim \frac{L}{d^2}. \quad (14)$$

The self energy contribution of a straight step can be adjusted to be the same as the line energy of a DGSOS model. Because in this model both the line energy and the step interaction originate from eq. (12), their relative amplitude is fixed and we can concentrate on the crossover from a local to a long-range model depending on the cutoff length l . Note, however, that other relative amplitudes can in principle be obtained by a different choice of $\Psi(r)$ at small distances $r < 1$ in eq. (11).

The simulation is carried out on a square lattice of size $L^2 = 64 \times 64$ to 128×128 . In order to calculate the difference in energy for every metropolis Monte Carlo trial, we apply a multi-grid scheme based on²¹ which has already been applied successfully to submonolayer epitaxy²².

This cuts down the computational costs from order L^4 to order $L^2 \log(L)$ for each time-step, which has to be multiplied by an additional factor of L^2 , for the number of time-steps the system needs to equilibrate. Without the use of the multi-grid scheme the computational costs would not have permitted system sizes beyond $L = 25$. Still the system size, $L \leq 128$, is rather restricted and we are aware that the results should be accounted as qualitative rather than quantitative. However, computations on the DGSOS and ASOS models at $L = 128$, which we did for comparison, give transition temperatures $T_R \approx 1.5J$ and $T_R \approx 1.25J$ respectively, which agree reasonably well with known results²³.

IV. RESULTS

A. Height Correlation Function

We determine the roughening temperature T_R from the behavior of the height-height correlation function. Below roughening, $T < T_R$, the interface is macroscopically flat, i. e. the height-height correlation function

$$G(r) = \langle [h(0) - h(r)]^2 \rangle \quad (15)$$

approaches a finite value in the limit $r \rightarrow \infty$. To be more precise, the correlation length ξ is finite and the interface has a characteristic width. Approaching the transition temperature the correlation length increases

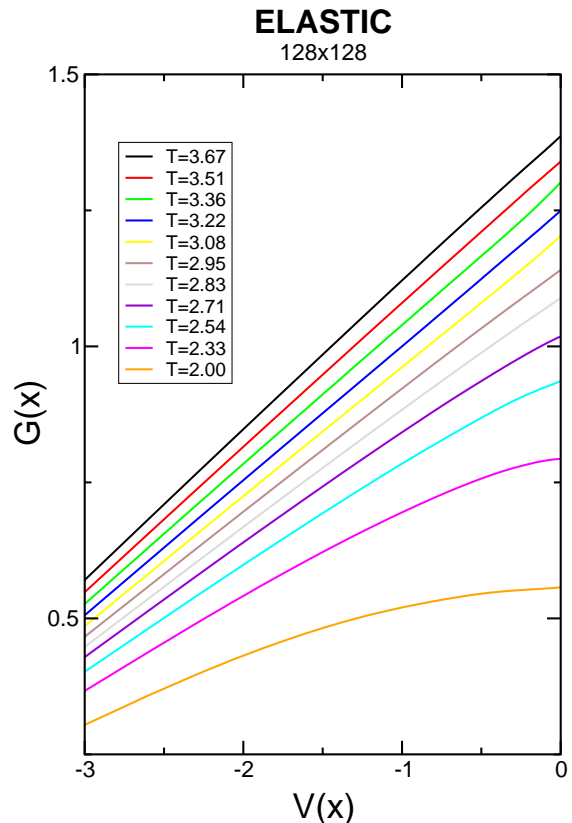


FIG. 2: Height-height correlation function without cutoff. The correlation function saturates for small temperatures and shows logarithmic behavior for $T > T_R$. The first straight line gives an estimate of $T_R \approx 2.8$.

and diverges at $T = T_R$. For $T > T_R$ the correlation function $G(r)$ diverges²³ according to the conventional theory of the roughening transition,

$$G(r) \sim K(T) \log r, \quad (16)$$

with an amplitude $K(T)$ depending on the temperature. Plotting $G(r)$ vs. $\log r$ one could determine at what temperature the correlation length ξ diverges and the graphs approach a straight line.

In a finite system with periodic boundary conditions, however, the correlation length ξ cannot exceed the system size L , the height-height correlation function $G(r)$ saturates for $T > T_R$ as well. In order to overcome this finite-size effect, we will use an approach similar to the one used in²⁴. In order to keep the argument simple we only consider correlations along the main directions of the lattice and replace r by x .

As the limiting behavior of $G(x)$ for periodic boundary conditions has to be a periodic function that behaves like the logarithm for distances $\ll L$, we define a “periodic logarithm” by means of Fourier analysis. In order to avoid the singularity at $r \rightarrow 0$ we start with

$$v(x) = \max(\log(x), 1) \quad (17)$$

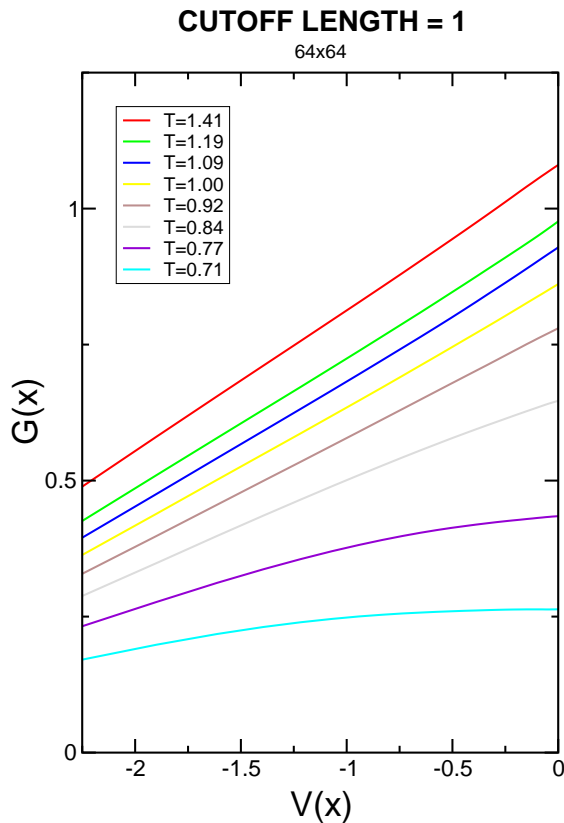


FIG. 3: Height-height correlation function with a cutoff length 1, i.e. only charges on nearest-neighbor-sites interact. The first straight line gives an estimate of $T_R \approx 0.9$.

and the integral-Fourier or, using symmetry arguments, the cosine transform

$$\tilde{v}(k) = \frac{1}{\pi} \int_0^{\infty} \cos(kx)v(x)dx. \quad (18)$$

Making use of these Fourier components we define the L -periodic function $V_L(x)$

$$V_L(x) = \frac{2\pi}{L} \sum_{n=1}^{\infty} \tilde{v} \left(\frac{2\pi n}{L} \right) \cos \left(\frac{2\pi n}{L} x \right) \frac{\sin \left(\frac{2\pi n}{L} \right)}{\frac{2\pi n}{L}}, \quad (19)$$

which is a discrete back transform averaged over unit distances. For convenience we define

$$V(x) = V_L(x) - V_L(L/2) \quad (20)$$

and plot $G(x)$ vs. $V(x)$. Fig. 2 shows the correlation function for the case of the full $1/r^3$ interaction. At a temperature of about $T = 2.8$ the graph becomes straight, indicating the roughening transition. Restricting the elastic dipole charge interaction to distances ≤ 1 , the graph of the correlation function becomes straight at a lower temperature $T = 0.9$, see Fig. 3.

From the Kosterlitz-Thouless theory of the roughening transition, the slope of the correlation function is

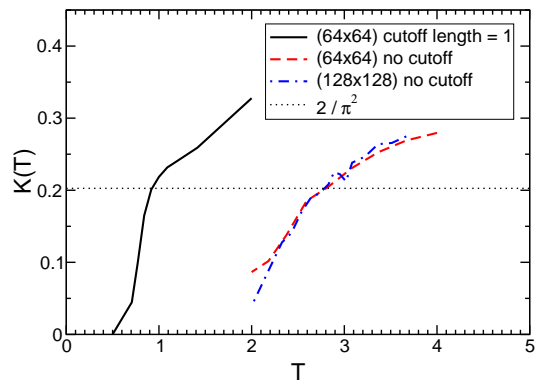


FIG. 4: Slope $K(T)$ vs. temperature. Estimation of T_R using the universal value from conventional roughening theory gives $T_R = 2.8$ for infinitely ranged interaction and $T_R = 0.9$ for cutoff length 1.

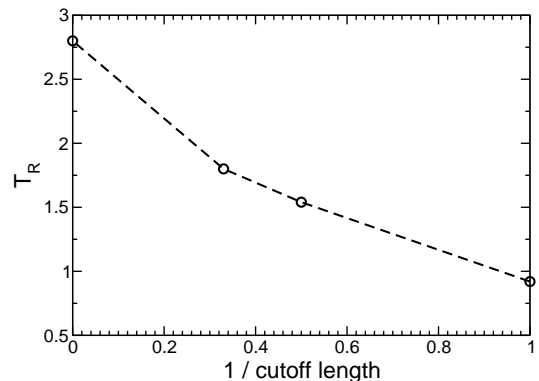


FIG. 5: Roughening temperature T_R vs. inverse cutoff length $1/l$. Even at $l = 3$ the roughening temperature $T_R \approx 1.8$ is well below the infinite range potential value.

expected to assume the universal value $K(T_R) = 2/\pi^2$. Plotting slope vs. temperature one can also obtain an estimate of the roughening temperature, see Fig. 4. From this we obtain identical estimates for the two cases with or without cutoff.

From this we conclude that the system with long-range interaction has a much higher transition temperature compared to the model with interaction cutoff, the roughening temperature changes by a factor ~ 3 .

Note that the roughening temperature increases gradually with the cutoff length, see Fig. 5. Even at $l = 3$ the roughening temperature $T_R \approx 1.8$ is still well below the value for infinite range interaction. The increase of the roughening temperature is not a next nearest neighbor effect.

B. Energetic Scales

One might argue that increasing the range of the interaction potential just changes the relevant energetic scale.

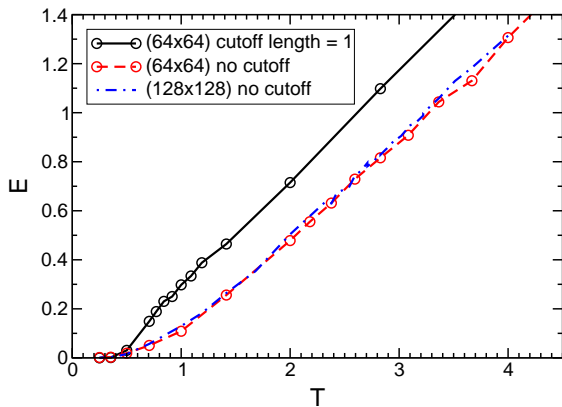


FIG. 6: Average energy per unit surface E vs. temperature T . Average energy for the cutoff-potential is strictly higher in comparison to the long-range case.

However, the energetic scales one is usually tempted to think of, i.e. the energy of a straight step or single kinks on such a step, do not change by more than 36%. The straight line energy per unit step length increases from $w_l = 0.39$ to 0.53, the corresponding kink energy changes from $w_k = 0.88$ to 1.18. In the low temperature regime, the energy of one single ad-atom on a flat crystal surface is the important energetic scale, which changes from $w_a = 2.53$ to 2.69, an increase by no more than 6%.

It should be noted that the main contribution to the change of these energetic scales comes from short-range interactions. Using a cutoff length of $l = 3$, the straight line and kink energies are only about 6 – 7% below the full potential value, whereas the single ad-atom defect energy deviates by no more than 0.05%.

From the change of these energetic scales one usually would expect an equal increase of the roughening temperature. One would hesitate, however, to make these changes responsible for an increase of the roughening temperature by a factor of ~ 3 .

C. Average Energy

Comparing the average energy E of the system computed with and without restriction of the charge interaction range, one clearly sees that the energy for the non restricted interaction always stays well below the graph of the restricted system, see Fig. 6. For high temperatures the average energy E goes linear with temperature T , indicating that the heat capacity becomes constant.

The range of the interaction potential only affects the behavior below the transition temperature. Above the roughening transition all details of the interaction are combined into one single parameter, the roughening temperature T_R . Accordingly the scaled graphs E/T_R vs. T/T_R coincide for $T/T_R > 1$, see Fig. 7.

The decrease in average energy of the system using long-ranged interaction coincides with a smaller number

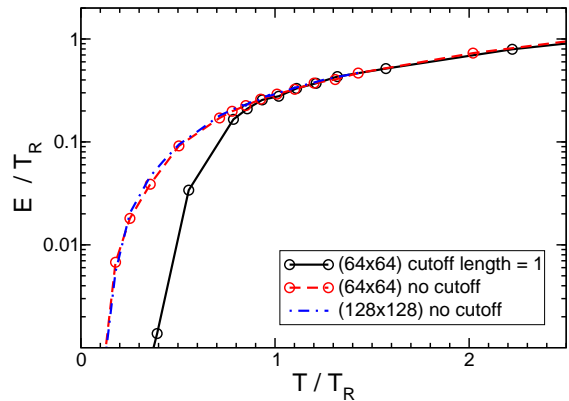


FIG. 7: Scaled average energy per unit surface E vs. scaled temperature T/T_R . For $T/T_R \geq 1$ the scaled data collapses onto a single graph.

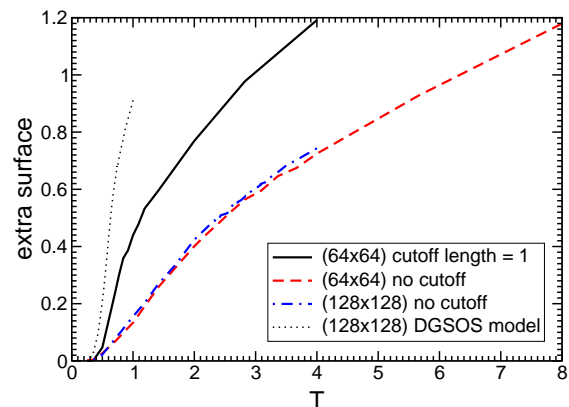


FIG. 8: Extra surface, i.e. number of broken bonds, vs. temperature T . Fewer defects are created when no cutoff is used.

of broken bonds, see Fig. 8. The number of deviations from a facet or the step length is smaller compared to the system with interaction potential cutoff.

D. Defect Correlations

Restricting the surface height to $\{-1, 0, +1\}$, one may talk about a defect wherever the height deviates from the average height 0. Then one can analyze correlation between these defects, i.e. the thermal average of

$$g_{\text{defect}}(r) = \frac{\langle [h^2(\mathbf{r}') - h^2(\mathbf{r}' + \mathbf{r})]^2 \rangle_{\mathbf{r}'}}{\langle h^2(\mathbf{r}') \rangle_{\mathbf{r}'}}. \quad (21)$$

Scaled like this, the defect correlation will approach the value 1 for large distances r . At low temperatures repulsion between the defects causes the graph to fall below value 1 at midrange distances and ends well above value 1 at distance $r = 1$, because contact between equal defects is favored due to what might be called surface or

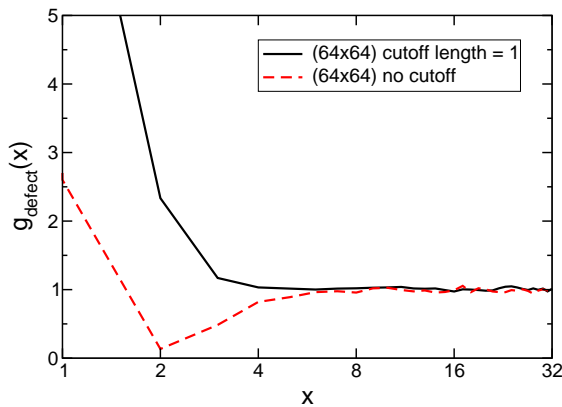


FIG. 9: Defect correlation at $T = 0.5$ for both long-range interaction and cutoff. The long-range interaction causes a stronger repulsion gap (here near $x = 2$), which means that the defects prefer to be separated. This anti-correlation effect is responsible for a strong decrease in entropy.

line energy. Increasing the temperature, this repulsion gap will become smaller and vanish eventually.

Fig. 9 shows the defect correlation for both long-range interaction and cutoff for identical temperature. Whereas for long-range interaction the gap is still present, it has already vanished from the system with cutoff. The pronounced repulsion gap in the case of the infinite range interaction means that a single defect or island avoids being close to other defects. This cuts down the number of favorable configurations and thus reduces the entropy contribution to the free energy for given density of defects n .

For the following argument we will assume that the main result is a reduction of entropy by some factor

$\alpha < 1$, whereas the average energy at given n remains unchanged. In a rather simplified picture we can then write the free energy like $F_\alpha = E(n) - T\alpha S(n)$, where n depends on temperature T and is determined by $\partial F/\partial n = 0$. In this picture the free energy $F_\alpha(T)$ of the system with reduced entropy at temperature T has the same properties as the original system at a lower temperature αT . Thus if the original system had a roughening temperature T_R the transition temperature \tilde{T}_R of the system with reduced entropy will increase to $\tilde{T}_R = T_R/\alpha$.

V. CONCLUSION

In summary, we have presented a model which contains the essential effects of long-range elastic repulsion between steps on a crystal surface. We conclude that correlations due to these long-range interactions can strongly increase the roughening temperature in solid-on-solid models, mainly by a reduction of the entropy. Since defects prefer to exist in secluded areas, the number of favorable configurations and consequently the entropy contribution to the free energy is diminished, leading to an increase of the roughening temperature. Our simulations suggest that the type of transition remains the same, although a rigorous proof lies beyond the scope of this type of Monte Carlo approach.

Acknowledgments

The authors would like to thank V.I. Marchenko for valuable comments and suggestions.

-
- ¹ J. M. Kosterlitz and D. J. Thouless, *J. Phys. C* **6**, 1181 (1973).
 - ² S. T. Chui and J. D. Weeks, *Phys. Rev. B* **14**, 4978 (1976).
 - ³ J. M. Kosterlitz, *J. Phys. C* **7**, 1046 (1974).
 - ⁴ J. M. Kosterlitz, *J. Phys. C* **10**, 3753 (1977).
 - ⁵ T. Ohta and K. Kawasaki, *Prog. Theor. Phys.* **60**, 365 (1978).
 - ⁶ H. J. F. Knops and L. W. J. Ouden, *Physica A* **103**, 597 (1980).
 - ⁷ P. J. M. Bastiaansen and H. J. F. Knops, *Phys. Rev. B* **53**, 126 (1996).
 - ⁸ M. den Nijs, *Phys. Rev. Lett.* **64**, 435 (1990).
 - ⁹ E. Jagla, S. Prestipino, and E. Tosatti, *Phys. Rev. Lett.* **83**, 2753 (1999).
 - ¹⁰ G. Mazzeo, G. Jug, A. C. Levi, and E. Tosatti, *Phys. Rev. B* **49**, 7625 (1994).
 - ¹¹ J. D. Noh and M. den Nijs, *J. Phys. A* **30**, 7375 (1997).
 - ¹² S. Prestipino, G. Santoro, and T. Erio, *Phys. Rev. Lett.* **75**, 4468 (1995).
 - ¹³ D. L. Woodraska and J. A. Jaszczak, *Phys. Rev. Lett.* **78**, 258 (1997).
 - ¹⁴ A. Prasad and P. B. Weichmann, *Phys. Rev. B* **57**, 4900 (1998).
 - ¹⁵ A. Andreev and Y. Kosevich, *Sov. Phys. JETP* **54**, 761 (1981).
 - ¹⁶ V. Marchenko and A. Parshin, *Sov. Phys. JETP* **52**, 129 (1980).
 - ¹⁷ J. Hardy and R. Bullough, *Phil. Mag.* **15**, 237 (1967).
 - ¹⁸ V. M. Kaganer and K. H. Ploog, *Phys. Rev. B* **64** (2001).
 - ¹⁹ T. W. Poon, S. Yip, P. S. Ho, and F. F. Abraham, *Phys. Rev. Lett.* **65**, 2161 (1990).
 - ²⁰ T. W. Poon, S. Yip, P. S. Ho, and F. F. Abraham, *Phys. Rev. B* **45**, 3521 (1992).
 - ²¹ J. Steinbrecher, H. Müller-Krumbhaar, E. Brener, C. Misbah, and P. Peyla, *Phys. Rev. E* **59**, 5600 (1999).
 - ²² F. Gutheim, H. Müller-Krumbhaar, and E. Brener, *Phys. Rev. E* **63** (2001).
 - ²³ J. Lapujoulade, *Surf. Sci. Rep.* **20**, 191 (1994).
 - ²⁴ Y. Saito and H. Müller-Krumbhaar, *Phys. Rev. B* **23**, 308 (1981).